

Hybrid 28 GHz MMW over fiber-wireless QPSK transmission system based on mid L-band external injection-locked quantum-dash laser comb source

Q. Tareq^a, A.M. Ragheb^b, E. Alkhazraji^c, M.A. Esmail^d, S. Alshebeili^{b,e}, M.Z.M. Khan^{a,*}

^a Optoelectronics Research Laboratory, Electrical Engineering Department, King Fahd University of Petroleum and Minerals, Dhahran 31261, Saudi Arabia

^b KACST-TIC in Radio Frequency and Photonics for the e-Society (RFTONICS), King Saud University, Riyadh 11421, Saudi Arabia

^c Electrical and Electronics Engineering Technology Department, Jubail Industrial College, Jubail 31961, Saudi Arabia

^d Communications and Networks Engineering Department and Smart Systems Engineering Laboratory, Prince Sultan University, Riyadh 11586, Saudi Arabia

^e Electrical Engineering Department, King Saud University, Riyadh, Saudi Arabia

ARTICLE INFO

Keywords:

Quantum-dash laser
Millimeter waves
L-band optical communication
Ultra-narrow linewidth
Radio-over-fiber

ABSTRACT

We report on the generation and transmission of millimeter-wave (MMW) beat-tone at 28 GHz from an external injection-locked InAs/InP quantum-dash laser-based comb source emitting in mid L-band. The MMW beat-tone exhibited a narrow linewidth, and low phase noise of ~ -122 dBc/Hz at 1.0 MHz offset frequency, thus demonstrating superior characteristics. Thereafter, we achieved a successful transmission of 2 Gbps quadrature-phase-shift-keying (QPSK) signal over 28 GHz MMW beat-tone carrier on 4 m wireless channel as well as 20 km single-mode fiber and 4 m wireless hybrid channel, exhibiting receiver sensitivities of -1.0 and -0.5 dBm, respectively. This demonstration paves the way for the potential deployment of this new-class of MMW photonic source in future passive optical networks and 5G, enabling exploiting hybrid architectures and extended L-band wavelength operation besides the conventional C-band.

1. Introduction

The exponential proliferation of smart devices has significantly intensified the demand for mobile data traffic, projected to reach 77 Exabytes per month by 2022, a staggering sevenfold increase compared to 2017 [1]. To mitigate this demand, a fifth-generation New Radio (5G NR) wireless mobile network has been developed to enhance ubiquitous interconnectivity by offering ultra-reliable and low latency communications, enhanced mobile broadband, ultra-fast data transfer, and support applications such as high-definition video streaming, autonomous driving, teleconferencing, internet of things, etc. [2,3]. The future 5G wireless technology has been envisioned to provide data rates of Gigabits per second for subscribers and employing millimeter-wave (MMW) frequency band from 20 to 30 GHz, as suggested by 5G Public Private Partnership [4], since below 6 GHz window is already congested by the wireless services [5]. Although MMW suffers from significant signal fading owing to high atmospheric attenuation, the seamless integration with the existing fiber-to-the-x (FTTX) architecture for last-mile access can realize the delivery of ultra-broadband wireless signals, which is also termed as radio-over-fiber (RoF) technology. Moreover, hybrid RoF and wireless technologies are being considered as potential frontiers for

next-generation networks, and deploying 28–39 GHz range MMW band signals [6], which are garnering recent attention owing to their smaller free-space propagation loss compared to 60 GHz high-frequency bands, would be a promising solution to address the future needs.

For efficient high-speed mobile communication, the two most critical factors are optical generation and transmission of MMW, which has already been given considerable regard as a strong contender for 5G and RoF because traditional digitized electronic system impedes network scaling due to high complexity, low spectral efficiency and larger size [7]. Owing to this, microwave photonics has been extensively utilized to generate MMW signals in the optical domain. Among various techniques demonstrated in the literature, optical heterodyning is the most investigated that relies on beating two optical wavelengths from a comb source, or dual-wavelength laser, or two free-running laser diodes, at a photodiode [5]. In general, deploying free-running lasers gives rise to broadened MMW beat-tone linewidth (Δf_L) and high phase noise (S_ϕ) due to incoherency between the two optical wavelength modes. Therefore, techniques such as optical phase-locked loops [8] and injection-locking [9] have been employed on the optical source for successful spectral synchronization and purification of the heterodyned MMW carrier [6] with ultra-narrow Δf_L (full width at half maximum) and low

* Corresponding author.

E-mail address: zahedmk@kfupm.edu.sa (M.Z.M. Khan).

<https://doi.org/10.1016/j.yofte.2021.102553>

Received 23 January 2021; Received in revised form 18 March 2021; Accepted 9 April 2021

Available online 27 April 2021

1068-5200/© 2021 Elsevier Inc. All rights reserved.

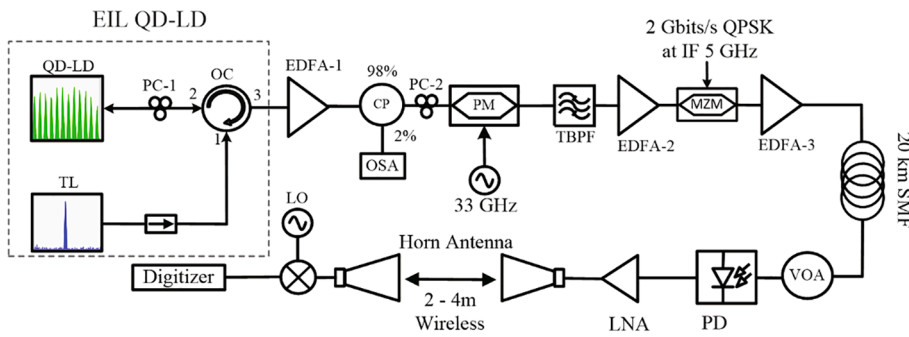


Fig. 1. Experimental setup for the generation and transmission of MMW beat-tone over the hybrid fiber-wireless channel. PC: polarization controller, QD-LD: quantum-dash laser diode (slave laser), TL: external tunable laser (master laser) OC: optical circulator, EDFA: Erbium-doped fiber amplifier, CP: optical coupler, TBPF: tunable bandpass filter, OSA: optical spectrum analyzer. PM: phase modulator, VOA: variable optical attenuator, PD: photodiode, ESA: electrical signal analyzer, AWG: arbitrary waveform generator, LNA: low-noise amplifier, MZM: Mach-Zehnder modulator, LO: local oscillator.

phase noise, which are imperative for high-performance transmission [3,10]. To achieve this, optical laser sources based on quantum-dash (QD), which are quasi-zero dimensional nanostructures, are attracting much attention as potential contenders in the MMW domain owing to their superior static and dynamic characteristics and noise, in particular, compared to their quantum-well counterpart [11,12]. Moreover, the QD emission spanning S- to L-band region makes QD laser diodes (QD-LD) promising MMW sources, seamlessly integrating with the existing optical network infrastructure and potentially satisfying extended L-band wavelength operation in future optical networks with hybrid architectures that are under serious consideration. Besides, QD-LD's multi-wavelength lasing emission nature could also be exploited in future MMW RoF-WDM systems wherein a single device may supply dual optical carriers to several L-band channels.

In the following, we provide a brief review of QD laser diode (QD-LD) deployment in the MMW domain, which is concentrated only in the C-band wavelength-operating window. Reference [13] reported the generation of 3–20 GHz microwave/MMW beat-tone with $\Delta f_L < 1$ MHz using dual-wavelength (DWL) QD distributive-feedback (DFB) laser. Subsequently, in [11], the generation of 146 GHz MMW signal and wireless transmission of 1.0 Gbps non-return-zero (NRZ) on-off keying (OOK) data is reported utilizing the QD-LD at ~ 1550 nm. On another front, in [14], fixed 50–60 GHz and tunable up to 98 GHz MMW signals were generated using a passive mode-locked (PMLL) ~ 1550 nm QD-LD with demonstrated $\Delta f_L < 18$ kHz, and $S_\phi -70$ dBc/Hz at 10 kHz offset frequency. Successful transmission of a 3.0 Gbps quadrature amplitude modulated (QAM) signal on a 60 GHz MMW carrier was demonstrated on an optimized PMLL QD-LD with $\Delta f_L \sim 10$ kHz [15]. In reference [3,16], generation of 46 and 48 GHz MMW signal from DWL QD-LD with $\Delta f_L \sim 26$ kHz and data transmission of 2.0 Gbps 4-level pulse amplitude modulation (PAM-4) was reported, while in [17] 1.17 Gbps over 25 km SMF using orthogonal frequency division multiplexing (OFDM) over 60 GHz MMW carrier was demonstrated employing QD-LD PMLL. Recently, generation of 40/80 GHz [20] and 50/100 GHz [21] using QD-LD

operating at 1550 nm and transmission over hybrid 50 km SMF and 10/20 m wireless link have been demonstrated. Unfortunately, reports in the L-band wavelength region for MMW applications are very limited; for instance, we recently exploited this wavelength domain to demonstrate a tunable dual-wavelength-mode generation with ~ 62 GHz free-spectral range and the possibility of tuning the mode spacing for tunable frequency MMW beat-tones in optical domain [22].

In this work, we report 28 GHz MMW beat-tone signal generation employing InAs/InP QD-LD operating at ~ 1610 nm, which is in the extended L-band window. External injection locking (EIL) scheme is utilized to realize a high spectral purity single locked Fabry–Pérot (FP) longitudinal mode and subsequent generation of optical comb in extended L-band region. This is to ascertain spectral synchronization of the filtered dual-comb lines and purification of the heterodyned 28 GHz MMW beat-tone carrier. Hence, narrow Δf_L and S_ϕ as low as ~ -122 dBc/Hz at 1 MHz offset frequency has been achieved. Moreover, we also demonstrate an error-free transmission of 2 Gbps QPSK signal on this 28 GHz MMW carrier over 4 m wireless and hybrid 20 km SMF – 4 m wireless channels and emphasize the potential of hybrid network architectures for future deployment. To our knowledge, this is the first report to demonstrate modulated MMW transmission in mid L-band employing EIL QD-LD over hybrid-channels. Moreover, our work further substantiates the potential of QD-LD as a candidate MMW source in future L-band RoF multiplexed passive optical networks while integrating hybrid channels for last-mile access applications [19].

2. Experimental details

In this work, we employed a bare 800 μm cavity length and 4 μm ridge width InAs/InP QD-LD with four stack quantum-dash chirped barrier thickness active region. Further details of the device structure can be found in [18]. The experimental setup developed for the photonic generation, transmission, and characterization of MMW beat tone is illustrated in Fig. 1. Firstly, the bare unbounded QD-LD is placed on a

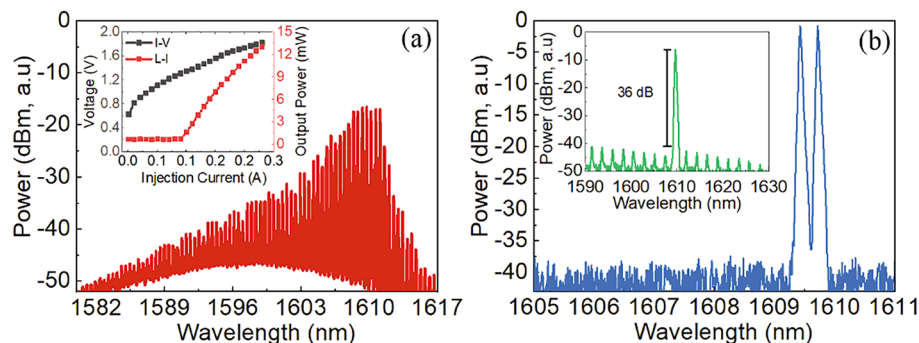


Fig. 2. (a) Free-running (un-locked) lasing spectrum of QD-LD riding on the ASE of EDFA-1 with the inset depicting the light output–injected current–bias voltage (L-I-V) characteristics. (b) Filtered dual-mode comb line from the comb source exhibiting identical peak power and 33 GHz free spectral range with inset showing the external injection-locked single-mode at ~ 1610 nm with 36 dB SMSR.

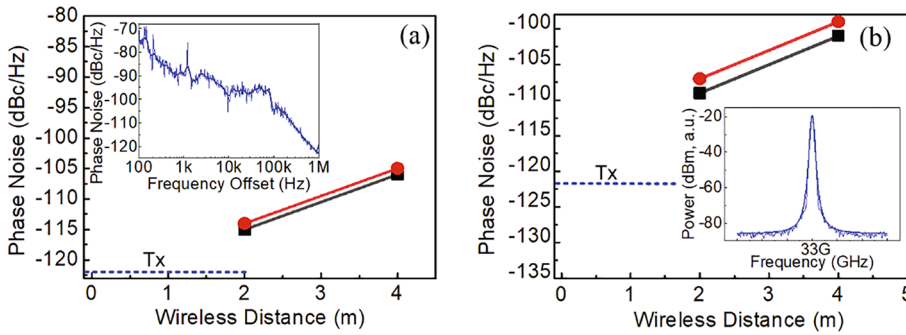


Fig. 3. Phase noise S_ϕ characteristics of 28 GHz modulated (red symbols) and 33 GHz unmodulated (black symbols) MMW carrier at 1.0 MHz offset frequency, as a function of wireless link length for (a) wireless and (b) hybrid channels, measured at the receiver end with an error margin of ± 2 dBc/Hz. The insets of (a) and (b) shows the electrical spectrum and the S_ϕ curve of 33 GHz MMW unmodulated carrier measured at the transmitter side. The Tx dotted line in (a) and (b) corresponds to the phase noise measured at the transmitter side. (For interpretation of the references to colour in this figure legend, the reader is referred to the web version of this article.)

temperature-controlled brass base (TEC, Keithley 2510) to ensure the lasing wavelength emission within the operating wavelength limitations of optical equipments and components. The device is manually mounted and probed with a continuous wave (CW) current using Keithley 2520. The optical power was measured using an InGaAs photodiode with a calibrated integrating sphere, and the resulting light-current-voltage (I - V) characteristics are depicted in the inset in Fig. 2 (a), exhibiting a threshold current (I_{th}) of ~ 90 mA and the near-threshold slope efficiency is ~ 0.13 W/A. Next, the optical power from a single as-cleaved facet of the FP laser is butt-coupled into an in-house made lensed SMF by manually tuning a three-axis translational stage, achieving a coupling efficiency of $\sim 5\%$. The operating current throughout the experiment is fixed at ~ 110 mA ($1.22I_{th}$) with 0.5 mW fiber-coupled power.

The next part of the setup corresponds to the EIL arrangement where the free-running QD-LD broadband lasing emission is connected to port 2 of an optical circulator (OC) via polarization controller (PC-1). The output from port 3 of the OC is amplified by an Erbium-doped fiber amplifier (EDFA-1, Amonics AEDFA-L-18BR) and passed to 98/2% optical coupler (CP) from where 98% port is the available output. The resulting free-running amplified broadband lasing spectrum, depicted in Fig. 2 (a), is obtained via an optical spectrum analyzer (OSA, Agilent 86142B) with 60 pm resolution connected to 2% of CP-1 before locking. Next, a commercial tunable laser (TL, Agilent 81600B) was employed as a master laser to external injection-lock a single longitudinal mode from the free-running spectrum by connecting to port 1 of the OC via an isolator to be fed into the QD-LD active region. The resultant external injection-locked single-mode at 1609.7 nm is depicted in the inset of Fig. 2 (b), obtained at an injection ratio of ~ -10 dB, and exhibiting a side mode suppression ratio (SMSR) of ~ 36 dB. It is to be noted that throughout this work, the injection ratio is fixed owing to the maximum optical power limit of the TL, and the EDFA-1 is deployed to compensate for the coupling loss of QD-LD optical power into the SMF.

In the subsequent arrangement, the externally injection-locked mode is fed through PC-2 to a phase modulator (PM, Eospace 40 GHz) driven by a 33 GHz electrical signal (Keysight E8267D PSG). The PM's output is a seven-mode comb achieved by creating three harmonics on each side of the locked mode with 33 GHz mode spacing. It is noteworthy to mention here that the comb source mode spacing can be altered to generate tunable MMW frequencies by adjusting the radio frequency (RF) signal's frequency. Next, a tunable bandpass filter (TBPF) was utilized to filter two comparable peak power comb lines, as depicted in Fig. 2 (b), exhibiting an optical signal-to-noise ratio (OSNR) of ~ 36 dB. The modes' peak power was aligned with PC-2 and then amplified to ~ 15 dBm using EDFA-2 (AEDFA-L-EX2-B-FA) to compensate for the PM and TBPF insertion losses (~ 10 – 12 dB). These dual modes are then externally modulated with a 2 Gbps QPSK signal using a single drive Mach-Zehnder (MZM) modulator. The baseband QPSK signal was generated in MATLAB by mapping a pseudo-random binary sequence (PRBS) pattern with a length of $2^{11}-1$ using an arbitrary waveform generator (AWG, Keysight M8190A with 6 GHz bandwidth) at 12 GSa/s, which was offset to an intermediate carrier frequency (IF) of 5 GHz,

thereby essentially translating to 28 GHz MMW transmitted carrier that is of interest in this work (neglecting other higher frequency MMW beat-tones while some of them will be filtered out by low noise amplifier, LNA (operating bandwidth ~ 24 – 40 GHz), before wireless transmission). The modulated dual optical modes are further amplified to compensate for the MZM insertion loss before transmitting over a 20 km SMF.

The modulated optical dual-mode signal from the receiving end of the SMF is then converted into an electrical MMW signal by beating the modes in a 70-GHz bandwidth photodiode (PD, Finisar XPDV3120R) after passing through a variable optical attenuator (VOA, Agilent N7764A), which serves to investigate the transmission performance. The modulated MMW carrier is further amplified using LNA before transmitting over horn antennas (26 – 40 GHz bandwidth and 25 dB gain) that are placed 0–4 m apart, thus corresponding to hybrid channel (20 km SMF and 0–4 m wireless). The received electrical MMW signal from this hybrid channel is then down-converted by mixing with a local oscillator (LO) at 28.5 GHz and then demodulated and analyzed using Keysight 12-bit digitizer (M9730B, bandwidth 1.2 GHz) operating at 3.4 GSa/s. We realized a wireless channel transmission system by removing the SMF from the system (Fig. 1) while keeping the remaining components intact. For the MMW beat-tone performance analysis at the receiver side, we placed the electrical spectrum analyzer (ESA, Keysight N9010B EXA) after the receiver horn antenna. On the other front, for the transmitter analysis in the case of the hybrid channel, we removed the SMF and connected ESA directly after the PD.

3. Results and discussion

This section presents the RF characteristics and transmission performance of the generated MMW beat-tone signal via the EIL QD-LD comb source. For this, two-channel configurations have been considered viz. a wireless channel with a variable distance of 0–4 m (space between the horn antennas) and a hybrid channel consisting of an additional 20 km SMF and the 0–4 m wireless channel. Moreover, for long-distance coherent optical communications, it is imperative that the MMW carrier possess very narrow Δf_L and S_ϕ below -100 dBc/Hz at 1 MHz offset [23], and even more so while a phase-sensitive modulation scheme, QPSK in our case, is being employed. Thus, to analyze and understand the impact of transmission as well as modulation on the RF characteristics, we measured Δf_L and S_ϕ of the MMW beat-tone at the transmitter as well as receiver end for both unmodulated 33 GHz and modulated 28 GHz carrier. We selected an offset frequency of 1 MHz and plotted the measured S_ϕ values for the wireless and hybrid channels in Fig. 3 (a) and (b), respectively, with an error margin of ± 2 dBc/Hz. Moreover, S_ϕ characteristics, measured at the transmitter side, are shown in the inset of Fig. 3 (a). The unmodulated 33 GHz exhibited a value of ~ -122 dBc/Hz at the transmitter side, degraded to ~ -115 (-106) dBc/Hz after 2 (4) m wireless transmission, as depicted in Fig. 3 (a). Considering the modulated 28 GHz MMW carrier, not much change in S_ϕ is observed (difference of ± 1.0 dBc/Hz) compared to the unmodulated 33 GHz carrier. This is an expected observation since the

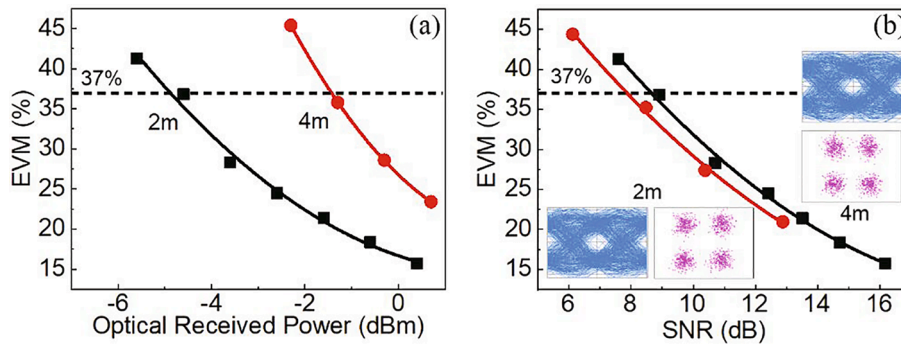


Fig. 4. Transmission performance of EIL QD-LD comb source generated 28 GHz MMW carrier for a wireless link length of 2 and 4 m. (a) EVM versus the received optical power, and (b) EVM versus the received average SNR. The insets in (b) correspond to the received QPSK constellation and eye diagram at a fixed ~ 10 dB SNR for 2 m (bottom) and 4 m (top) wireless link lengths. The horizontal dotted lines correspond to the 37% EVM FEC limit.

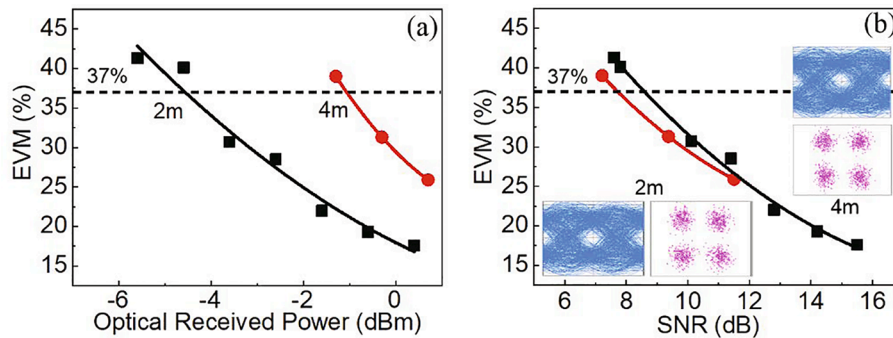


Fig. 5. Transmission performance of EIL QD-LD comb source generated 28 GHz MMW carrier for the hybrid channel of 20 km SMF and 2–4 m wireless distance. (a) EVM versus the received optical power (b) EVM versus the received average SNR. The insets in (b) correspond to the received QPSK constellation and eye diagram at a fixed ~ 10 dB SNR for 2 m (bottom) and 4 m (top) wireless link length of the hybrid channel. The horizontal dotted lines correspond to the 37% EVM FEC limit.

modulated carrier is essentially derived from the unmodulated carrier. Upon further addition of a 20 km SMF along with the wireless distance for the hybrid channel case (Fig. 3(b)), we notice an increase in S_ϕ values. In this case, the unmodulated carrier degraded by an average value of ~ 6.0 dBc/Hz compared to the wireless channel counterpart, while the S_ϕ of modulated carrier follows that of the unmodulated carrier, again showing consistency of the measurements. We attribute this inferior S_ϕ on including the SMF to the walk-off effect due to fiber chromatic dispersion that may reduce the coherency of dual-modes, thereby increasing the random phase noise of the MMW carrier [24,26]. Moreover, comparing the 2 m and 4 m wireless links for both channels, a decrease in S_ϕ by ~ 4.0 dB/Hz/m is noted, which may be ascribed to possible RF fading [25] which could be due to reflections from the edges of the receiving antenna, thus affecting the phase noise. Subsequently, we extracted Δf_L from the electrical spectrum of the 33 GHz unmodulated (shown in the inset of Fig. 3(b) at the transmitter side) and 28 GHz modulated carrier at the receiver side. The spectrums are Lorentzian fitted to extract the Δf_L values for both channels and at various wireless channel lengths and observed to be in few kHz range, which is very narrow and highly stable when observed for a long time.

Next, we evaluate the transmission performance of the 28 GHz modulated MMW carrier generated by the EIL QD-LD by demodulating and signal processing at the receiver and measuring the error-vector magnitude (EVM) and SNR at different received optical power values that we alter using the VOA. In our case, the successful QPSK transmission is evaluated by sufficient EVM and average SNR of 37% and 8.5 dB, respectively [26], which translates to a BER of 3.8×10^{-3} . We investigate 2 Gbps QPSK signal transmission performance over both wireless and hybrid channels by varying the wireless link length and the received optical power. The corresponding measured results are plotted in Figs. 4 and 5. Considering the wireless channel, Fig. 4 (a) shows that

the EVM for 2 m wireless distance degraded from 15.8 to 41.5% on attenuating the received optical power from 0.4 to -5.6 dBm, while the EVM of 4 m wireless distance degraded from 23.5 to 45% when the received power is reduced from 0.7 to -2.3 dBm. Hence, for the successful transmission of 37%, the minimum required optical power, or in other words, the receiver sensitivity of ~ -5.0 and ~ -1.5 dBm, are noted for the 2 and 4 m wireless channel distances, respectively. Moreover, we substantiate this observation by plotting EVM as a function of SNR in Fig. 4(b) that shows SNR of 8.5 ± 0.25 dB at 37% EVM value, in good agreement with the desired value [26]. We attribute the degradation in receiver sensitivity to the additional RF free space path loss encountered by the longer wireless distance that also fades the received SNR. For instance, at a fixed received power of 0 dBm, the EVM of 2 (4) m wireless channel is noted to be 16.6 (27) %, and the corresponding measured average SNR is 15.6 (10.6) dB, thereby accounting for ~ 5 dB decrease in SNR. The insets of Fig. 4(b), which plots the received constellation and eye diagrams at a fixed SNR of ~ 10 dB, corresponding to $\sim 29\%$ EVM, for the 2 m and 4 m link distance, essentially does not show any penalty and exhibits an almost indistinguishable performance with clear cluster separation and an open eye.

Finally, we summarize the performance of hybrid 20 km SMF with 2–4 m wireless channel in Fig. 5(a) as a function of received optical power. In this case as well, 2 m wireless link showed EVM degradation from 17 to 42.6% when the received power is attenuated from 0.4 to -5.6 dBm, while for 4 m wireless link showed an increase of 26 to 39% when the optical power is reduced from 0.7 to -1.3 dBm. This translates to a receiver sensitivity of ~ -4.5 and ~ -1.0 dBm for the 2 and 4 m wireless length hybrid channels, which is ~ 0.5 dB inferior to the wireless channel case. We attribute this to additional chromatic dispersion-induced power fading distortion in the transmission channel due to the addition of SMF. Nevertheless, at 0 dBm received power, the

received average SNR faded by approximately the same value of ~ 5 dB, from 15 dB to 10 dB, on increasing the wireless link length from 2 m to 4 m, with a corresponding reduction of EVM from 18 to 29%, as depicted Fig. 5 (b). The QPSK constellation and eye diagrams, shown in the insets of Fig. 5(b), for the case of 10 dB SNR, again demonstrate clear open eye and well-separated constellations for both wireless channel lengths and affirms consistency of our measurements.

4. Conclusion

In summary, we realized a high-quality photonic generation of MMW beat-tone at 28 GHz, with a narrow Δf_L , employing an external injection-locked QD-LD based comb at ~ 1610 nm for future high-speed hybrid optical network infrastructures that are capable of potentially exploiting the extended L-band wavelength of operation. We demonstrated a successful QPSK signal transmission at 2 Gbps over 4 m wireless and 20 km SMF – 4 m wireless hybrid channels with system exhibited S_ϕ of ~ -105 and ~ -100 dBc/Hz at 1 MHz offset frequency, respectively. Moreover, we performed a comprehensive analysis of the 28 GHz MMW beat-tone carrier's generation and transmission performance, suggesting maximum power fading due to wireless free-space path rather than from the SMF. Thus, with this work, we strongly believe in mid L-band InAs/InP QD-LD as a potential candidate MMW photonics source for 5G and next-generation optical networks.

CRedit authorship contribution statement

Q. Tareq: Investigation, Data curation, Writing - original draft, Writing - review & editing, Visualization, Formal analysis. **A. M. Ragheb:** Methodology, Investigation, Resources, Writing - review & editing. **E. Alkhazraji:** Investigation, Writing - review & editing. **M. A. Esmail:** Investigation, Writing - review & editing. **S. Alshebeili:** Resources, Writing - review & editing. **M. Z. M. Khan:** Conceptualization, Methodology, Resources, Writing - original draft, Writing - review & editing.

Declaration of Competing Interest

The authors declare that they have no known competing financial interests or personal relationships that could have appeared to influence the work reported in this paper.

Acknowledgments

QT and MZMK acknowledge the support from King Fahd University of Petroleum and Minerals through grant SB181003. AMR and SAA thank the National Plan for Science, Technology, and Innovation (MAARIFAH), King Abdulaziz City for Science and Technology, Kingdom of Saudi Arabia, Award Number (2-17-02-001-0009). MAE acknowledges the support from Prince Sultan University.

References

- [1] Cisco. Cisco visual networking index: Forecast and trends 2017-2022 White Paper, 2019.
- [2] ETSI, 5G; Study on scenarios and requirements for next generation access technologies, Tech. Rep. v. 15.0.0, 2018.
- [3] M. Rahim, et al., Monolithic InAs/InP quantum dash dual-wavelength DFB laser with ultra-low noise common cavity modes for millimeterwave applications, *Opt. Express* 27 (2019) 35368–35375.
- [4] A. Gupta, R.K. Jha, A Survey of 5G Network: Architecture and Emerging Technologies, *IEEE Access* 3 (2015) 1206–1232.
- [5] L. Vallejo, et al., Impact of Thermal-Induced Turbulent Distribution Along FSO Link on Transmission of Photonically Generated mmW Signals in the Frequency Range 26–40 GHz, *IEEE Photonics J.* 12 (1) (2020) 1–9. Art no. 5500309.
- [6] H. Wang, C. Cheng, C. Tsai, Y. Chi, G. Lin, Multi-Color Laser Diode Heterodyned 28-GHz Millimeter-Wave Carrier Encoded With DMT for 5G Wireless Mobile Networks, *IEEE Access* 7 (2019) 122697–122706.
- [7] C. Han, M. Sung, S. Cho, H. Seok Chung, S.M. Kim, J.H. Lee, Performance Improvement of Multi-IFoF-Based Mobile Fronthaul Using Dispersion-Induced Distortion Mitigation With IF Optimization, *J. Lightwave Technol.* 34 (20) (2016) 4772–4778.
- [8] U. Gliese, T.N. Nielsen, S. Nirskov, K.E. Stubkjær, Multifunctional fiber-optic microwave links based on remote heterodyne detection, *IEEE Trans. Microwave Theory Technol.* 46 (5) (May 1998) 458–468.
- [9] L. Goldberg, H.F. Taylor, J.F. Weller, D.M. Bloom, Microwave signal generation with injection-locked laser diodes, *Electron. Lett.* 19 (13) (Jun. 1983) 491–493.
- [10] J. Yao, *Microwave photonics*, *J. Lightwave Technol.* 27 (3) (Feb. 2009) 314–335.
- [11] M.J. Fice, E. Rouvalis, F. van Dijk, A. Accard, F. Lelarge, C.C. Renaud, G. Carpintero, A.J. Seeds, 146-GHz millimeter-wave radio-over-fiber photonic wireless transmission system, *Opt. Express* 20 (2) (2012) 1769.
- [12] Q. Tareq et al., Tunable 28-60 GHz Millimeter Wave Signal Generation using L-band Quantum-dash Laser, Conference on Lasers and Electro-Optics Pacific Rim (CLEO-PR), Sydney, Australia, 2020, pp. 1-3.
- [13] F. van Dijk, et al., Monolithic dual wavelength DFB lasers for narrow linewidth heterodyne beat-note generation, in: International Topical Meeting on Microwave Photonics jointly held with the Asia-Pacific Microwave Photonics Conference, Singapore, 2011, pp. 73–76.
- [14] F. van Dijk et al., Quantum dash mode-locked lasers for millimeter wave signal generation and transmission, 23rd Annual Meeting of the IEEE Photonics Society, Denver, CO, 2010, pp. 187-188.
- [15] R. Rosales et al., InAs/InP quantum dash based mode locked lasers for 60 GHz radio over fiber applications, International Conference on Indium Phosphide and Related Materials, Santa Barbara, CA, 2012, pp. 185-187.
- [16] K. Zeb et al., Photonic Generation of Spectrally Pure Millimeter-Wave Signals for 5G Applications, International Topical Meeting on Microwave Photonics (MWP), pp. 1-4, Oct. 2019.
- [17] A. Delmade, T. Veroleto, C. Browning, Y. Lin, G. Aubin, F. Lelarge, A. Ramdane, and L. P. Barry, Quantum Dash Passively Mode Locked Laser for Optical Heterodyne Millimeter-Wave Analog Radio-over-Fiber Fronthaul Systems, in Optical Fiber Communication Conference (OFC) 2020, OSA Technical Digest (Optical Society of America, 2020), paper W2A.41.
- [18] M.Z.M. Khan, T.K. Ng, B.S. Ooi, Self-assembled InAs/InP quantum dots and quantum dashes: Material structures and devices, *Progr. Quantum Electron.* 38 (6) (2014) 237–313.
- [19] M.Z.M. Khan, et al., Injection-Locked Quantum-Dash Laser in Far L-Band 192 Gbit/s DWDM Transmission, *IEEE Photonics J.* 12 (5) (2020) 1–11. Art no. 1504211.
- [20] K. Mallick, et al., Generation of 40 GHz/80 GHz OFDM based MMW source and the OFDM-FSO transport system based on special fine tracking technology, *Optical Fiber Technol.* 54 (2020).
- [21] G.C. Mandal, R. Mukherjee, B. Das, A.S. Patra, A full-duplex WDM hybrid fiber-wired/fiber-wireless/fiber-VLC/fiber-IVLC transmission system based on a self-injection locked quantum dash laser and a RSOA, *Opt. Commun.* 427 (2018) 202–208.
- [22] E. Alkhazraji, et al., Hybrid Dual-injection Locked 1610 nm Quantum-dash Laser for MMW and THz Applications, *Opt. Commun.* 452 (March 2019) 355–359.
- [23] J. Beas, G. Castanon, I. Aldaya, A. Aragon-Zavala, G. Campuzano, Millimeter-Wave Frequency Radio over Fiber Systems: A Survey, *IEEE Commun. Surv. Tutorials* 15 (4) (2013) 1593–1619.
- [24] X. Li, J. Xiao, N.D.J. Yu, W-band vector millimeter-wave signal generation based on phase modulator with photonic frequency quadrupling and precoding, *J. Lightwave Technol.* 35 (13) (2017) 2548–2558.
- [25] X. Pang, A. Lebedev, J. Olmos, I. Monroy, Multigigabit W-band (75–110 GHz) bidirectional hybrid fiber-wireless systems in access networks, *J. Lightwave Technol.* 32 (23) (2014) 4585–4592.
- [26] C. Tsai, et al., 60-GHz Millimeter-wave Over Fiber with Directly Modulated Dual-mode Laser Diode, *Sci. Rep.* 6 (2016).